Diverse bacteriohemerythrin genes of *Methylomonas denitrificans* FJG1 provide insight into the survival and activity of proteobacterial methanotrophs under hypoxia

Running Title: Bacteriohemerythrin genes in methanotrophs

Cerrise Weiblen[1], Dominic Sauvageau[2], Lisa Y. Stein[1#]

[1]Department of Biological Sciences, University of Alberta, Edmonton AB, Canada

[2]Department of Chemical and Materials Engineering, University of Alberta, Edmonton AB, Canada

Correspondence:

lisa.stein@ualberta.ca

Abstract word count: 201

Importance statement word count: 134

Main text word count: 4086

Abstract

Proteobacterial methanotrophic bacteria are dependent on the oxidation of methane and methanol for the assimilation of carbon. Interestingly, these types of methanotrophs can thrive in oxygen-depleted zones of lakes and other aquatic ecosystems despite the fact they are considered obligate aerobes. Bacteriohemerythrin (Bhr), a homologue of eukaryotic hemerythrin, is a protein associated with oxygen binding. The model gammaproteobacterial methanotrophic strain, *Methylomonas denitrificans* FJG1, oxidizes methane at the expense of nitrate reduction under extreme hypoxia and upregulates *bhr* genes, yet this strain encodes 10 homologues of *bhr* in its genome. Using *M. denitrificans* FJG1 as a model, this study examined the prevalence and phylogeny of each of its 10 *bhr* homologues in other methanotroph and general bacterial genomes. One gene copy denoted as "*bhr*-00" was found to be methanotroph-specific, was upregulated under hypoxia in *M. denitrificans* FJG1, and was predicted to have a structure nearly identical to the crystalized, oxygen-scavenging, Bhr-Bath protein from, *Methylococcus capsulatus* Bath. Other upregulated *bhr* genes from hypoxic cultures of nitrate-grown *M. denitrificans* FJG1 included those with gene neighborhoods related to oxygen sensing, denitrification and chemotaxis. Together, this study uncovered multifunctional roles of bacteriohemerythrin proteins encoded and expressed by methanotrophs that likely enable their survival in hypoxic ecosystems.

Importance

Aerobic gammaproteobacterial methanotrophs encoding bacteriohemerythrin (*bhr*) genes are reported to have an enhanced ability to survive and grow in oxygen-limited environments. The methanotrophic bacterium, *Methylomonas denitrificans* FJG1, encodes 10 copies of *bhr* genes, of which 7 are expressed under oxygen depleted and denitrifying conditions. Comparing

these 10 *bhr* gene homologues from *M. denitrificans* FJG1 with those from other prokaryotic genomes revealed that copy "*bhr-00*" is nearly exclusive to methanotrophs. Gene neighbourhoods surrounding conserved *bhr* gene sequences in methanotroph genomes suggest a range of potential functions including oxygen sensing and delivery, chemotaxis, and nitrate reduction. The results from this study illuminate a previously undescribed diversity of the structure and function of *bhr* genes in *M. denitrificans* FJG1 and related methanotrophic bacteria and pinpoints roles of Bhr that likely promote survival of methanotrophs in hypoxic ecosystems.

Introduction

Hemerythrin (Hr) and its bacterial homologue, bacteriohemerythrin (Bhr), is a multifunctional and structurally diverse protein family linked to many metabolic functions in eukaryotes and prokaryotes, including reactive oxygen and nitrogen species (ROS/RNS) detoxification, metal ion detoxification, iron storage, transmembrane signaling, oxygen sensing, chemotaxis, biofilm formation, cellular respiration, and oxygen binding and transport (1, 2). The functional diversity of Hr and Bhr proteins places them at the crossroads between metabolic pathways, even within a single organism, and previous research has shown that genetically similar Hr and Bhr enzymes can perform an array of different functions. For instance, Baert et al. (3) identified Hr from the leech *Theromyzon tessulatum* which was classified as an iron storage molecule named "ovohemerythrin." In bacterial systems, Kendall et al. (4) investigated the functions of three Bhr homologues in the bacterium *Campylobacter jejuni*: one had a protective role in preventing molecules with iron-sulfur clusters (Fe-S) from incurring oxygen damage, and the other two were related to flagellar biosynthesis and expression of sigma-factor 28. In the bacterium *Neanthes diversicolour*, a Bhr was found associated with cadmium detoxification functions (5). Research from Xiong et al. (6) showed that the oxygen-sensitive bacterium *Desulfovibrio vulgaris* used a Bhr-like protein as an oxygen sensor with a role in chemotaxis. French et al. (7) showed that Bhr in *Vibrio cholerae* was part of the cyclic-di-GMP signaling system with involvement in biofilm formation. And last, Chen et al. (8) showed that Bhr in *Phascolopsis gouldii*, described as myohemerythrin, was involved in oxygen storage and transport.

Several reports of Bhr proteins in gammaproteobacterial methanotrophs, aerobic bacteria that use methane as a primary energy and carbon source, have emerged in recent years. A survey of *bhr* homologues identified in methanotroph genomes showed that 80% of strains possessed at

least one and up to three *bhr* gene copies (9). The model strain, *Methylococcus capsulatus* Bath, was found to use Bhr to supply oxygen to methane monooxygenase, and a crystal structure of this protein was also resolved (10-12). In *Methylotuvimicrobium alcaliphilum* 20Z, Nariya et al. (13) showed that overexpression of Bhr supported aerobic respiration but did not enhance methane oxidation capacity under low oxygen. However, in the model organism *Methylomonas denitrificans* FJG1, transcripts of *bhr* were among the most highly expressed under hypoxic conditions, along with genes for methane oxidation and denitrification to support its respiration under low oxygen (14). For this reason, *M. denitrificans* FGJ1 was selected as the model organism for the current study as methane-dependent respiration of nitrate was initially characterized in this strain and *bhr* was identified one of the most highly expressed genes in supporting its physiology (14). From the above studies, the role of Bhr for methanotrophs appears to be primarily the binding and delivery of oxygen, perhaps because O_2 is an essential substrate for particulate methane monooxygenase (pMMO) to oxidize methane to methanol; there is no alternative oxidant yet known to enable this activity *in vivo*. However, aerobic methanotrophs are capable of using alternate terminal electron acceptors (TEAs), such as nitrate (14), nitrite (15) and iron oxides (16), even though oxygen remains their preferred TEA.

While Bhr appears to be important to methanotroph physiology, particularly regarding oxygen binding, the diversity, distribution and potential multifunctionality of Bhr across methanotroph species is unknown. The present study investigates the phylogeny of 10 Bhr homologues identified in the *M. denitrificans* FJG1 genome, identification of two paralogous *bhr* genes that appear specific to gammaproteobacterial methanotroph lineages, speculated functions of Bhr for hypoxic survival based on gene neighbourhoods, differential expression of *bhr* and neighboring genes by *M. denitrificans* FJG1 when grown with high or low oxygen levels and with ammonium or nitrate, and predicted structures of the 10 Bhr proteins of *M. denitrificans*

FJG1. Together, this work illuminates previously unknown diversity of *bhr* genes and proteins possessed and expressed by *M. denitrificans* FJG1 and how a variety of Bhr functions likely enable gammaproteobacterial methanotrophs to occupy extremely hypoxic niches.

Results

Phylogeny of *bhr* genes identified in *Methylomonas denitrificans* FJG1. The methanotrophic bacterium *Methylomonas denitrificans* FJG1 encodes 10 *bhr* homologues annotated as "hemerythrin family," "hemerythrin domain-containing protein," or "bacteriohemerythrin" (Table 1). The genes, numbered *bhr*-00 through *bhr*-99, were designated based on their proximity to the origin of replication in the *M. denitrificans* FJG1 genome sequence (Supplemental Fig. S1). Eight of the 10 *bhr* genes are approximately 400 bp, typical of the oxygen-carrying Bhr protein originally discovered in eukaryotes (2), whereas *bhr*-66 is approximately 1,000 bp and *bhr*-55 is approximately 4,000 bp (Table 1). BLASTn searches were performed with each of the 10 *bhr* genes to identify homologues across methanotrophic and non-methanotrophic bacteria. Candidate genes from these BLASTn searches were then aligned to a concatenated sequence of the 10 *bhr* homologues (separated by 100 bp spacers to prevent mismatching) of *M. denitrificans* FJG1. The best alignments of candidates to one of the *bhr* genes from *M. denitrificans* FJG1 were used to generate a unified phylogeny for all 10 homologues (Fig. 1). The resulting unrooted phylogram of positive matches revealed that *bhr*-66 is the most common bacteriohemerythrin-containing gene among a diverse assemblage of microorganisms (Fig. 1). In contrast, *bhr*-00 and *bhr*-99 appear nearly exclusive to methanotrophs in the *Methylococcales* order, with few identified in non-methanotroph genomes. Closer examination of complete *bhr* genes from methanotroph genomes revealed that *bhr*-00 and *bhr*-66 homologues were the most common, but only *M. denitrificans* FJG1 encoded *bhr*-11, *bhr*-

33, *bhr*-44 and *bhr*-55 among the proteobacterial methanotrophs (Fig. 1; Supplemental Data, Sheet 3).

As *bhr*-66 was the most common bacteriohemerthyrin homologue found among bacteria, we examined its detailed phylogeny with organisms for which full genomes were available (Fig. 2; Supplemental Data, Sheet 3). A cladogram using full-length *bhr*-66 alignments showed its polyphyletic distribution, several instances of horizontal gene transfer, and a range of annotations (e.g. histidine kinase, response regulator, hypothetical protein) that suggest a relationship to the Bhr class of oxygen-sensing and signal transducing types (17) (Fig. 2). Expectedly, *bhr*-66 was monophyletic for the methanotrophic bacteria. We compared the phylogeny of methanotroph *bhr*-66 genes with their 16S rRNA genes and found that they were highly congruent, suggesting a long-term vertical transmission (Fig. 3). Similar congruence was found for the methanotroph-specific *bhr*-00 gene. When comparing phylogenies between *bhr*-00 and *bhr*-99, their high congruence and sequence similarity suggests that the two genes are possible paralogues (Fig. 3). Similarly, two pairs: *bhr*-33/-44, and *bhr*-77/-88 share high sequence similarity to one another, suggesting that these pairs of genes may also be paralogues (Supplemental data sheet 3). The *bhr*-77/-88 genes are encoded contiguously, perhaps due to a recent gene duplication event, and thus share the same gene neighbourhood. As very few genomes encode *bhr*-11, -22, -33, -44, -77 and -88, we could not perform a detailed phylogenetic analysis of these genes across bacterial or methanotroph species.

Conservation and predicted functions of *bhr* gene neighbourhoods in methanotrophic bacteria. To explore the possible functionalities of the commonly shared *bhr* genes among the methanotrophic bacteria, we compared the surrounding gene neighbourhoods for *bhr*-00, -66 and -99 among several methanotroph genomes (Fig. 4). The *bhr*-00 gene neighbourhood is highly conserved among the *Methylomonas* and *Methylotuvimicrobium* genera

and the *bhr*-00 gene is flanked by operons for biotin synthesis (*bio*BFHCD), an enzyme co-factor, and cytochrome *c* oxidase (*cox*/*cta*) used for oxygen respiration. The *bhr*-66 gene neighbourhood is less well conserved, with genes related to signal transduction (i.e. response regulator) and ATP-binding domains flanking *bhr*-66 in most *Methylomonas* genomes, and genes for the electron carrying cytochrome P-460 flanking *bhr*-66 in *Methylmicrobium* and *Methylotuvimicrobium* genomes (Fig. 4). Although *bhr*-99 appears to be a paralogue of *bhr*-00, its gene neighbourhood is distinct and conserved in four of the *Methylomonas* genomes (Fig. 4). For these genomes, the gene encoding the AlkB DNA-repair enzyme is encoded on the same DNA strand as *bhr*-99. An operon for the Na^+-translocating NADH:quinone oxidoreductase (NQR) complex, which is involved in creating sodium motive force for transporter and flagellar function (18), is encoded on the opposing strand. The upstream region of *bhr*-99 is not conserved among methanotroph genomes (Fig. 4).

Differential expression of *bhr* and neighboring genes in *M. denitrificans* FJG1 when grown under hypoxia. To determine which *bhr* genes are highly expressed by *M. denitrificans* FJG1 under hypoxia, we examined differential expression of the 10 *bhr* homologues and their surrounding gene neighbourhoods under oxic (24 h) and hypoxic (48 h) conditions when grown in either ammonium (AMS) or nitrate (NMS) mineral salts media (14). Among the *bhr* genes, only *bhr*-00 showed a significant (>2 norm log2 ratio) increase in expression under hypoxic conditions in either media (Fig. 5, Table 2). This gene was also, by orders of magnitude, the most highly expressed homologue among the *bhr* genes. Even though *M. denitrificans* FJG1 only denitrifies when grown in NMS medium, the AMS-grown bacteria also differentially expressed *bhr*-00 to the same magnitude (Table 2), indicating that hypoxia, and not N-source, was the signal affecting its expression. Five of the other *bhr* homologues (*bhr*-11, -55, -66, -77, -88) only showed significantly increased expression ($P<0.05$) under hypoxia when *M. denitrificans* FJG1

was grown in NMS, but not AMS medium, suggesting a linkage to denitrification functions (Fig. 5, Table 2).

Genes encoding the enzymes for nitrate reduction were in the gene neighbourhood of *bhr*-11 and all showed significantly increased expression under hypoxia for only NMS-grown cells (Fig. 5, Table 3). This result was expected as *M. denitrificans* FJG1only denitrifies in the presence of nitrate (14). The gene neighbourhood of *bhr*-66 showed increased expression for ATP-binding cassette and response regulator genes in cells grown only in NMS medium, suggesting potential involvement of these genes in oxygen sensing under denitrifying conditions (Table 3). Furthermore, the gene neighbourhood for *bhr*-77/-88 that includes multiple genes for chemotaxis showed significant upregulation under hypoxia for *M. denitrificans* FJG1 grown only in NMS medium, suggesting that chemotaxis-related functions are also connected to the denitrifying phenotype of *M. denitrificans* FJG1 (Table 3).

Diversity of Bhr protein structures from *M. denitrificans* FJG1. As the 10 *bhr* genes of *M. denitrificans* FJG1 vary in size and genomic context, we further explored their diversity using AlphaFold2 to predict their putative protein structures (Fig. 6A). Each predicted structure showed unique features, although Bhr-33 and Bhr-44 were highly similar to one another. When the structure of Bhr-00 was overlaid with the experimentally derived structure of the Bhr-Bath protein, an oxygen binding and delivery system (8), the structures were largely congruent, even though their nucleotide identities overlap by 61.44% (Fig. 6B; Supplemental Fig. S2; Supplemental movie). Thus, based on its similar structure, the location of conserved histidine residues, and coordination of its diiron cofactor, the function of Bhr-00 is likely the same as that of Bhr-Bath.

The hybrid structure of Bhr-66 helps explain the inconsistency in its gene annotation and phylogeny (Fig. 2). The predicted Bhr-66 structure of *M. denitrificans* FJG1 shows a distinct

bacteriohemerythrin structure of four alpha-helices arranged in a chimney shape at the N-terminus, which was the segment likely identified by BLAST as a bacteriohemerythrin gene. The bacteriohemerthyrin domain is appended by a linear C-terminal extension containing two structures with distinctive folds reminiscent of PAS domains of s-box histidine kinases and response regulators, suggesting that Bhr-66 likely acts as part of an oxygen-sensing two-component regulatory system that has been well described previously (1, 19, 20). This may also explain the proximity of genes annotated as response regulators in the neighbourhoods of some methanotroph *bhr*-66 genes (Fig. 4) Similarly, the predicted Bhr-55 structure appears to have a bacteriohemerythrin segment at the N-terminus with a long trailing section comprising the C-terminus, which includes up to seven folded PAS-like domains. As sequences related to *bhr*-55 were not identified in other genomes, further analysis regarding its evolution, phylogeny and function were not pursued.

Discussion

Methylomonas denitrificans FJG1 consumes methane and reduces nitrate to survive in under extreme hypoxia (14). This bacterium was shown to significantly increase its expression of *bhr* under denitrifying conditions, which presumably allowed it to bind oxygen in the cytoplasm to support continued methane oxidation and respiration (10). Close examination of the *M. denitrificans* FJG1 genome revealed 10 homologues of *bhr* genes, but it was not clear which gene was responsible for supporting respiration, methane oxidation, and growth of *M. denitrificans* FJG1 under hypoxia. The present study provided a detailed examination of the phylogeny, gene neighbourhood context, gene expression, and predicted protein structures of the 10 *bhr* gene homologues of *M. denitrificans* FJG1, and validated that Bhr-00, a bacteriohemerythrin that is nearly exclusive to gammaproteobacterial methanotrophs, is likely the oxygen-binding protein

responsible for supporting their continued methane oxidation, respiration and growth under extreme hypoxia. Moreover, *bhr* homologues associated with denitrification (*bhr*-11), oxygen sensing (*bhr*-66), and chemotaxis (*bhr*-77, -88) were identified in *M. denitrificans* FJG1 and showed increased expression only under denitrifying conditions.

The hemerythrin originally discovered in marine worms, Hr, is encoded by a ~ 400 bp gene that produces a ~ 100-amino acid monomer that assembles into an octameric oxygen transport protein, causing the pink hue of the worms' blood (2). The Bhr-Bath protein purified from *M. capsulatus* Bath crystallized as a monomer and was shown to enhance oxygen delivery from the cytoplasm to pMMO-enriched intracytoplasmic membranes (10-12). Purified Hr and Bhr-Bath proteins turned an opaque reddish-purple or bright pink colour when exposed to O_2 (11, 21) which is the same colour as *M. denitrificans* FJG1 cells, and other *Methylomonas* isolates, grown to stationary phase in liquid culture or on plates. Based on the extremely high level of *bhr*-00 expression in *M. denitrificans* FJG1, particularly under hypoxia, its conserved proximity to genes encoding cytochrome *c* oxidase, and the structural similarity of Bhr-00 to Bhr-Bath, it is highly likely that the Bhr-00 protein is responsible for binding O_2, leading to its pink colour and its promotion of methane oxidation and respiration under extreme hypoxia.

Some forms of hemerythrin bind to substrates other than oxygen, such as nitric oxide, as a defense mechanism (22, 23). Under hypoxic conditions, *M. denitrificans* FJG1 upregulates genes in the *bhr*-11 gene neighbourhood, which includes enzymes in the denitrification pathway, to produce nitrite and nitric oxide that can bind to Bhr, and thus perhaps to the co-expressed Bhr-11 protein. The relationship of Bhr proteins to chemotaxis functions, like Bhr-77/-88, have been observed in other bacteria as having oxygen-sensing functions (17, 22). Determining the specific function of Bhr proteins is hindered by artifacts from previous research methods, such as basing classifications on COG (clusters of orthologous genes) categories. Because bacteriohemerythrin

domain proteins are multifunctional, they are not specific to a particular COGs and have thus routinely been excluded from data sets that use COG designations. Additionally, hemerythrin genes for oxygen-transport (~ 400 bp) and sensory/chemotaxis (> 400 bp) functions are not well differentiated in the literature and are inconsistently annotated. The diversity of *bhr* genes expressed by *M. denitrificans* FJG1 illuminates the functional flexibility of bacteriohemerythrin domain proteins from those that only bind and transport oxygen to larger complexes involved in signal transduction. The complex regulation of the *bhr* homologues in *M. denitrificans* FJG1 (Fig. 5, Table 3) shows how an individual organism can use Bhr domain proteins for multiple functions from hypoxia to reactive nitrogen species (e.g. nitrate, nitrite).

This study revealed an exceptional number and diversity of *bhr* gene homologues in *M. denitrificans* FJG1 that is yet unmatched by other methanotroph genomes. Gammaproteobacterial methanotrophs, usually in the *Methylomonas* genus, are frequently found at relatively high population density in hypoxic to anoxic ecosystems, particularly freshwater lakes (Reis et al., unpublished review). It is tempting to speculate that expression of the methanotroph-specific *bhr*-00 is involved in their ability to oxidize methane under extremely low oxygen availability in natural ecosystems. Moreover, the apparent restriction of *bhr*-00 to few related genera (*Methylomonas*, *Methylotuvimicrobium*, *Methylomicrobium*) could explain the enrichment of these particular phylotypes in oxygen-limited ecosystems that support methane oxidation.

Materials and Methods

Phylogenetic analyses. The genome sequence of *M. denitrificans* FJGI (GenBank accession CP014476A) was downloaded and analyzed using Geneious Prime 2019 (v1.2.3). The *M. denitrificans* FJG1 genome was found to contain 10 coding sequences (CDS) annotated as

hemerythrin, bacteriohemerythrin, hemerythrin family or hemerythrin domain-containing proteins in the GenBank and RefSeq annotation databases (Table 1). To facilitate further analyses, the 10 sequences were designated *bhr*-00 through *bhr*-99 in the order of location from the genome origin of replication for the purposes of this study.

Unrooted phylogrammatic overview of *M. denitrificans* FJG1 *bhr* homologues using BLASTn hits from prokaryote genomes. Phylogenetic analyses of the 10 *bhr* sequences from *M. denitrificans* FJG1 were performed using Geneious Prime 2019 (v1.2.3). The BLAST plug-in was used with default settings, except word size was decreased to 11 and a maximum return of 5,000 sequences was chosen. The resulting dataset was filtered by excluding eukaryotic organisms and prokaryotic organisms containing fewer than two *bhr* BLASTn hits.) The resulting BLASTn hits were collected into a database and categorized by aligning them to a concatenated sequence consisting of the 10 *M. denitrificans* FJG1 genes separated by spacers of 100 base pairs. The concatenated reference sequence eliminates duplicate matches and ensures that BLASTn hits are correlated to the appropriate *M. denitrificans* FJG1 sequence with which they share the greatest sequence similarity (Supplemental Data, Sheet 3). An unrooted phylogram (Fig. 1) was generated to show an inclusive overview of *bhr* genes among prokaryotic genomes (Geneious Prime 1.2.3, Global alignment with free end gaps, Cost matrix 51% similarity (5.0/-3.0), Tamura-Nei, Neighbor-Joining, No Outgroup, Gap open penalty 12, Gap extension penalty 3, Automatically determine direction; Supplemental Data, Sheet 3).

The BLASTn hits were used to identify complete methanotroph genomes encoding putative *bhr* sequences. A circular alignment of these genomes was generated using BLAST Ring Image Generator (BRIGv0.95 default settings, Upper threshold 70%, Lower threshold 50%) to show the location of their *bhr* gene sequences in relation to each other (Accession numbers

CP014476, CP033381, CP023669, CP002738, CP014360, CP022129, CP035467, CP024202, CP046565, FO082060, NC_002977.6, AP017928; Supplemental Fig. S1).

The BLASTn hits were also used to identify full length CDSs including start and stop codons in all collected genomes. Full length *bhr* sequences were aligned using the Geneious Alignment tool (Global Alignment with free end gaps, Cost Matrix: 51%, default settings) and three rooted cladograms were generated using Geneious Prime 2019, one for each of the *M. denitrificans* FJG1 CDSs with matches in four or more genomes (total $n \geq 5$) (Geneious Tree Builder v1.2.3, Genetic Distance Model: Tamura-Nei, Tree Build Method: Neighbour-joining, Resampling Method: 1,000 bootstrap, Support Threshold: 50%, Image Scale: Substitutions per site). Cladograms for *bhr*-00 and *bhr*-99 in methanotroph genomes (Fig. 3) were rooted with the prokaryotic outlier, *Chitinomonas* sp. R3-44 (CP041730); however, in order to include all prokaryotes for the widely distributed *bhr*-66 sequence (Fig. 2), the cladogram was rooted using hemerythrin sequences from the eukaryote, *Themiste pyroides* (KY007473.1, KY007474.1, KY007475.1, KY007476.1, KY007477.1, KY007478.1, KY007479.1). For phylogenetic comparison, 16S rRNA trees were generated from representative genomes using the same methods. Comparative images were created using Geneious Prime 2019 and colour was added to highlight branch differences.

Identification and comparison of *bhr* gene neighbourhoods. Three of the 10 *bhr* sequences (*bhr*-00, *bhr*-66, and *bhr*-99) were selected for gene neighbourhood analysis, as at least five methanotroph genomes contained homologous copies to those found in *M. denitrificans* FJG1. Approximately 16,000 bp surrounding each *bhr* sequence was extracted from each annotated genome. Rather than relying on canonical reference sequences, in cases where multiple genomes were found for a species, the most recent annotated genome assembly was used to leverage the most up-to-date annotations. In cases where full genomes were found but lacked

gene annotations, they were annotated in-house using Geneious Prime 2019 (Default settings, Similarity > 50%), drawing from the in-house database of all annotated methylotroph genomes downloaded for this project (> 2,000 genomes). Comparative genomics based on these neighbourhood extractions was used to investigate the surroundings of each *bhr* sequence. Annotations were compared manually to overcome inconsistencies in labeling methodology. Colour schemes were used to identify sequences sharing similar or related functions while maintaining the annotation labeling of the original authors (Fig. 5). An accompanying comparison of the *bhr*-66 gene neighbourhood in non-methanotroph genomes is available in Supplemental Fig. S3.

Transcriptional analysis of *M. denitrificans* FJG1. The RNAseq experiment was performed as described by Kits et al. (14). Briefly, *M. denitrificans* FJG1 was cultured in 100 mL NMS or AMS medium (Whittenbury et al., 1970) in 250-mL sealed Wheaton bottles. 5 replicate cultures for each condition were inoculated with 1% v/v late-log phase culture of *M. denitrificans* FJG1 and provided with methane:air ratio of 3:7. Cultures were incubated at 30°C with shaking (200 rpm). Replicate cultures were sacrificed at 24 h (oxic) and 48 h (anoxic) (Supplemental Fig. S4) and cells were collected by filtration for RNA purification using the RNA Clean and Concentrator kit (Zymo Research, Irvine CA). rRNA depletion was accomplished with the Ribo-Zero rRNA Removal Kit (Epicentre, Madison WI) and RNA purity and concentration were confirmed using a Bioanalyzer 2100 (Agilent, Santa Clara CA) and the Quant-iT RNA assay kit (Invitrogen, Carlsbad, CA). TruSeq libraries were prepared using the RNA Sample Prep Kit v2 and sequenced on an Illumina HiSeq 2000 (Illumina). Output reads were trimmed and assessed for quality control prior to mapping against the *M. denitrificans* FJG1 genome using Geneious Prime 2019 (v1.2.3). The DESeq2 plug-in (default settings) was used to calculate expression values and differential expression. PCA plots were used to identify outliers with < 7% total

within-treatment variance; none were found, resulting in n=5 replications for each treatment (AMS 24 h, AMS 48 h, NMS 24 h, NMS 48 h). Differential expression comparing 24-h vs 48-h time points was calculated and applied to the neighbourhood maps for all 10 *bhr* sequences for cultures grown with NMS and AMS media (Figure 6 and Table 2). Transcriptome data can be found under GenBank accession number SRX696231.

Protein Structure Predictions. Predicted protein structures corresponding to the *bhr* gene loci for *M. denitrificans* FJG1 were downloaded from AlphaFold2 (alphafold.ebi.ac.uk) (24, 25). Nine structures were predicted that corresponded to Bhr-00 (A0A140E3I1), Bhr-11 (A0A140E4Z5), Bhr-22 (A0A126T104), Bhr-33 (A0A126T1L7), Bhr-44 (A0A126T494), Bhr-66 (A0A126T8C7), Bhr-77 (A0A126T8U2), Bhr-88 (A0A126T8Y8), and Bhr-99 (A0A140E6J4) (Fig. 4). The predicted structure of Bhr-66 was further investigated by extracting the hemerythrin section at the N-terminus and separating it from the C-terminal section of the gene into two nucleotide subsequences. The *bhr* domain (~400 nucleotides) and the C-terminal tail subsequence (~1,200 nucleotides) were used for BLASTn searches in the GenBank nucleotide database (Geneious Prime 2019, v1.2.3 with BLAST plugin, default settings, filtered by Grade > 40%) and the annotations from matching sequences were translated and examined for each subsection of the *bhr*-66 gene, revealing a hemerythrin domain at the N-terminus and a chain of multiple PAS sensing domains at the C-terminal end. No corresponding structure for Bhr-55 was available in the AlphaFold database, thus an alternative protein structure prediction tool was used (https://robetta.bakerlab.org/). The FASTA sequence of the *bhr*-55 gene was uploaded to the online tool and prediction was performed using RoseTTAFold, with default settings on the translated protein. The resulting visualization was coloured according to Error Estimate in the Robetta interface.

The predicted Bhr-00 (A0A140E3I1) structure and the Bhr-Bath structure (PDB ID: 4XPX) were downloaded from the RCSB Protein Data Bank (Berman et al. 2000) and imported into the MolStar Viewer (26) to compare their structures. Protein structures were superposed using a single Lys residue in each amino acid sequence (Lys 68, Bhr-Bath and Lys 70, Bhr-00). The Mol* animation is available in .mp4 format as a Supplemental Movie. The AA alignment of FJG1 Bhr-00 and Bhr-Bath is available as Supplemental Fig. S2.

Acknowledgments

This work was funded by the Canada First Research Excellence Fund in Future Energy Systems (D.S. and L.Y.S.), the Natural Sciences and Engineering Council of Canada Discovery Program (LYS), and the Mitacs Accelerate Program (D.S.). The funders had no role in the study design, data collection or interpretation, or in the decision to submit the work for publication.

C.W., D.S. and L.Y.S. participated in the planning of the study. C.W. performed the experiments, interpreted the data, and drafted the manuscript. D.S. and L.Y.S. provided financial support, critical analysis, writing and editing of the manuscript. All authors approved the manuscript for publication. The authors wish to thank K.D. Kits for providing RNAseq data for expression analysis.

This research was performed at the University of Alberta, located on the traditional territory of indigenous peoples and Métis that are part of Treaties 6, 7, and 8. We acknowledge, respect, appreciate, and support the sovereignty, lands, histories, languages, knowledge systems, and cultures of First Nations, Métis, and Inuit nations.

References

1. Alvarez-Carreño C, Alva V, Becerra A, Lazcano A. 2018. Structure, function and evolution of the hemerythrin-like domain superfamily. Protein Sci 27:848-860.
2. Costa-Paiva EM, Whelan NV, Waits DS, Santos SR, Schrago CG, Halanych KM. 2017. Discovery and evolution of novel hemerythrin genes in annelid worms. BMC Evol Biol 17.
3. Baert JL, Britel M, Sautiere P, Malecha J. 1992. Ovohemerythrin, a major 14-kDa yolk protein distinct from vitellogenin in leech. Eur J Biochem 209:563-569.
4. Kendall JJ, Barrero-Tobon AM, Hendrixson DR, Kelly DJ. 2014. Hemerythrins in the microaerophilic bacterium *Campylobacter jejuni* help protect key iron-sulphur cluster enzymes from oxidative damage. Environ Microbiol 16:1105-1121.
5. Demuynck S, Li KW, Vanderschors R, Dhainautcourtois N. 1993. Amino acid sequence of the small cadmium-binding protein (MP II) from *Nereis diversicolour* (annelida, polychaeta) - Evidence for a myohemerythrin structure. Eur J Biochem 217:151-156.
6. Xiong JJ, Kurtz DM, Ai JY, Sanders-Loehr J. 2000. A hemerythrin-like domain in a bacterial chemotaxis protein. Biochemistry 39:5117-5125.
7. French CE, Bell JML, Ward FB. 2008. Diversity and distribution of hemerythrin-like proteins in prokaryotes. FEMS Microbiol Lett 279:131-145.
8. Chen KHC, Chuankhayan P, Wu HH, Chen CJ, Fukuda M, Yu SSF, Chan SI. 2015. The bacteriohemerythrin from *Methylococcus capsulatus* (Bath): Crystal structures reveal that Leu114 regulates a water tunnel. J Inorg Biochem 150:81-89.
9. Rahalkar MC, Bahulikar RA. 2018. Hemerythrins are widespread and conserved for methanotrophic guilds. Gene Rep 11:250-254.
10. Chen KHC, Wu HH, Ke SF, Rao YT, Tu CM, Chen YP, Kuei KH, Chen YS, Wang VCC, Kao WC, Chan SI. 2012. Bacteriohemerythrin bolsters the activity of the particulate methane monooxygenase (pMMO) in *Methylococcus capsulatus* (Bath). J Inorg Biochem 111:10-17.
11. Kao WC, Wang VCC, Huang YC, Yu SSF, Chang TC, Chan SI. 2008. Isolation, purification and characterization of hemerythrin from *Methylococcus capsulatus* (Bath). J Inorg Biochem 102:1607-1614.
12. Karlsen OA, Ramsevik L, Bruseth LJ, Larsen O, Brenner A, Berven FS, Jensen HB, Lillehaug JR. 2005. Characterization of a prokaryotic haemerythrin from the methanotrophic bacterium *Methylococcus capsulatus* (Bath). FEBS J 272:2428-2440.
13. Nariya S, Kalyuzhnaya MG. 2020. Hemerythrins enhance aerobic respiration in *Methylomicrobium alcaliphilum* 20Z, a methane-consuming bacterium. FEMS Microbiol Lett 367.
14. Kits KD, Klotz MG, Stein LY. 2015. Methane oxidation coupled to nitrate reduction under hypoxia by the Gammaproteobacterium *Methylomonas denitrificans*, sp. nov. type strain FJG1. Environ Microbiol 17:3219-3232.
15. Kits KD, Campbell DJ, Rosana AR, Stein LY. 2015. Diverse electron sources support denitrification under hypoxia in the obligate methanotroph *Methylomicrobium album* strain BG8. Front Microbiol 6.
16. Li B, Tao Y, Mao ZD, Gu QJ, Han YX, Hu BL, Wang HW, Lai AX, Xing P, Wu QL. 2023. Iron oxides act as an alternative electron acceptor for aerobic methanotrophs in anoxic lake sediments. Water Res 234.
17. Kitanishi K. 2022. Bacterial hemerythrin domain-containing oxygen and redox sensors: Versatile roles for oxygen and redox signaling. Front Molec Biosci 9.
18. Barquera B. 2014. The sodium pumping NADH:quinone oxidoreductase (Na+-NQR), a unique redox-driven ion pump. J Bioenerg Biomembr 46:289-298.
19. Taylor BL, Zhulin IB. 1999. PAS domains: Internal sensors of oxygen, redox potential, and light. Microbiol Molec Biol Rev 63:479.
20. Yamada S, Sugimoto H, Kobayashi M, Ohno A, Nakamura H, Shiro Y. 2009. Structure of PAS-linked histidine kinase and the response regulator complex. Structure 17:1333-1344.

21. Stenkamp RE, Sieker LC, Jensen LH, McCallum JD, Sandersloehr J. 1985. Active site structures of deoxyhemerythrin and oxyhemerythrin. Proc Natl Acad Sci 82:713-716.
22. Alvarez-Carreño C, Becerra A, Lazcano A. 2016. Molecular evolution of the oxygen-binding hemerythrin domain. Plos One 11.
23. Nocek JM. 1986. The reactions of nitric oxide and nitrite with hemerythrin. PhD Thesis. Iowa State Univ. https://doi.org/10.31274/rtd-180813-13092.
24. Jumper J, Evans R, Pritzel A, Green T, Figurnov M, Ronneberger O, Tunyasuvunakool K, Bates R, Žídek A, Potapenko A, Bridgland A, Meyer C, Kohl SAA, Ballard AJ, Cowie A, Romera-Paredes B, Nikolov S, Jain R, Adler J, Back T, Petersen S, Reiman D, Clancy E, Zielinski M, Steinegger M, Pacholska M, Berghammer T, Bodenstein S, Silver D, Vinyals O, Senior AW, Kavukcuoglu K, Kohli P, Hassabis D. 2021. Highly accurate protein structure prediction with AlphaFold. Nature 596:583-589.
25. Varadi M, Anyango S, Deshpande M, Nair S, Natassia C, Yordanova G, Yuan D, Stroe O, Wood G, Laydon A, Zídek A, Green T, Tunyasuvunakool K, Petersen S, Jumper J, Clancy E, Green R, Vora A, Lutfi M, Figurnov M, Cowie A, Hobbs N, Kohli P, Kleywegt G, Birney E, Hassabis D, Velankar S. 2022. AlphaFold Protein Structure Database: massively expanding the structural coverage of protein-sequence space with high-accuracy models. Nucleic Acids Res 50:D439-D444.
26. Sehnal D, Bittrich S, Deshpande M, Svobodová R, Berka K, Bazgier V, Velankar S, Burley SK, Koča J, Rose AS. 2021. Mol* Viewer: modern web app for 3D visualization and analysis of large biomolecular structures. Nucleic Acids Res 49:W431-W437.

Data Availability Statement

Publicly available transcriptome datasets were analyzed in this study. This data can be found in GenBank (accession number SRX696231). The genomic datasets presented in this study can be found in online repositories. The names of the repositories and accession numbers can be found in the article and additional details are available in the Supplemental Data file.

Table 1. Classification of hemerythrin gene homologues in the genome of *Methylomonas denitrificans* FJG1 (Accession: CP014476).

Name	Locus_tag	GenomeStart	GenomeStop	Length	Direction	Gene Annotation	Protein_id	Protein Product	GO_function
bhr-00	JT25_RS00380	85767	85372	396	R	hemerythrin family protein	WP_036277397.1	bacteriohem-erythrin	GO:0046872 - metal ion binding
bhr-11	JT25_RS03015	663113	663445	333	F	hemerythrin domain-containing protein	WP_132325259.1	hemerythrin domain-containing protein	
bhr-22	JT25_RS04600	989403	989813	411	F	bacteriohemerythrin	WP_036273626.1	bacteriohem-erythrin	GO:0046872 - metal ion binding
bhr-33	JT25_RS05590	1204483	1204097	387	R	hemerythrin family protein	WP_036274438.1	hemerythrin family protein	
bhr-44	JT25_RS10375	2251509	2251123	387	R	hemerythrin family protein	WP_036280274.1	hemerythrin family protein	
bhr-55	JT25_RS11125	2420834	2416305	4530	R	bacteriohemerythrin	WP_062328608.1	bacteriohem-erythrin	GO:0046872 - metal ion binding
bhr-66	JT25_RS17815	3859160	3860944	1785	F	bacteriohemerythrin	WP_062329310.1	bacteriohem-erythrin	GO:0046872 - metal ion binding
bhr-77	JT25_RS18710	4064071	4063667	405	R	bacteriohemerythrin	WP_036274237.1	bacteriohem-erythrin	GO:0046872 - metal ion binding
bhr-88	JT25_RS18715	4064508	4064095	414	R	hemerythrin family protein	WP_036274239.1	bacteriohem-erythrin	GO:0046872 - metal ion binding
bhr-99	JT25_RS21450	4674029	4673625	405	R	hemerythrin family protein	WP_052142344.1	hemerythrin family protein	

Table 2. Differential expression of *bhr* gene homologues from *M. denitrificans* FJG1 based on RNAseq data collected after 24 and 48 h growth in NMS or AMS media with methane.

	Nitrate Treatment (NMS)					Ammonium Treatment (AMS)				
	Raw Expression (TPM)		Differential Expression 24h vs 48h			Raw Expression (TPM)		Differential Expression 24h vs 48h		
	24h	48h	log2 ratio	adjusted p-value	normalized log2 ratio	24h	48h	log2 ratio	adjusted p-value	normalized log2 ratio
bhr-00	4,657.50	13,150.82	1.35	0.000	3.33	7,706.16	28,626.86	1.91	0.000	3.21
bhr-11	38.22	62.58	0.47	0.034	2.45	75.47	23.55	-1.14	0.000	0.16
bhr-22	93.16	61.85	-0.65	0.000	1.33	122.98	57.33	-0.57	0.000	0.73
bhr-33	29.11	41.03	0.50	0.051	2.48	22.58	39.44	0.50	0.004	1.80
bhr-44	83.43	72.20	-0.28	0.104	1.70	74.32	65.09	-0.45	0.000	0.85
bhr-55	30.82	46.69	0.41	0.000	2.39	32.34	36.47	0.25	0.000	1.55
bhr-66	48.44	63.83	0.28	0.002	2.26	45.44	53.34	0.17	0.013	1.47
bhr-77	107.16	176.26	0.62	0.000	2.60	146.80	119.38	0.07	0.470	1.37
bhr-88	50.66	80.73	0.59	0.000	2.57	64.90	73.10	0.22	0.071	1.52
bhr-99	170.36	172.87	-0.05	0.732	1.93	193.38	181.93	-0.15	0.036	1.15
rpoB	418.02	113.34	-1.98	0.000		421.34	162.99	-1.30	0.000	

Table 3. Differential expression of neighboring genes upstream and downstream of the *bhr*-00, -11, -66, and -77/-88 homologues from *M. denitrificans* FJG1 based on RNAseq data at 24 h versus 48 h of growth in NMS and AMS media.

Gene name Abbreviation	Annotation	Genome Locus_tag	Gene Length	Direction	Nitrate Treatment (NMS)					Ammonium Treatment (AMS)				
					Raw Expression (TPM)		Differential Expression 24h vs 48h			Raw Expression (TPM)		Differential Expression 24h vs 48h		
					24h	48h	log2 ratio	adjusted p-value	norm log2 ratio	24h	48h	log2 ratio	adjusted p-value	norm log2 ratio
***bhr*-00 cytochrome *c* oxidase/biotin neighbourhood**														
	twin transmembrane helix small protein	JT25_RS00355	261	F	79.29	34.01	-1.09	0.000	0.89	125.15	56.68	-0.82	0.000	0.48
	cytochrome c oxidase subunit 3	JT25_RS00360	876	R	460.92	282.04	-0.75	0.000	1.23	392.14	388.57	0.16	0.000	1.46
	cytochrome c oxidase assembly protein	JT25_RS00365	543	R	1,941.07	1,120.97	-0.97	0.000	1.01	1,900.11	1,421.06	-0.33	0.000	0.98
ctaD	cytochrome c oxidase subunit I	JT25_RS00370	1617	R	1,103.57	597.90	-1.01	0.000	0.97	875.64	771.26	-0.19	0.000	1.11
coxB	cytochrome c oxidase subunit II	JT25_RS00375	1131	R	1,545.43	1,133.14	-0.60	0.000	1.37	1,458.49	1,556.46	0.07	0.000	1.37
bhr-00	hemerythrin family protein	JT25_RS00380	396	R	4,657.50	13,150.82	1.35	0.000	3.33	7,706.16	28,626.86	1.91	0.000	3.21
bioD	dethiobiotin synthase	JT25_RS00385	696	R	29.97	22.39	-0.38	0.071	1.60	23.62	25.97	-0.10	0.517	1.20
bioC	malonyl-ACP O-methyltransferase BioC	JT25_RS00390	789	R	30.27	24.52	-0.66	0.002	1.32	28.87	21.38	-0.29	0.041	1.01
bioH	pimeloyl-ACP methyl ester esterase BioH	JT25_RS00395	762	R	51.20	38.11	-0.66	0.000	1.32	76.59	36.15	-0.20	0.095	1.10
bioF	8-amino-7-oxononanoate synthase	JT25_RS00400	1161	R	34.95	33.30	-0.24	0.111	1.74	44.40	33.37	-0.13	0.220	1.17
bioB	biotin synthase BioB	JT25_RS00405	990	R	35.14	43.71	-0.07	0.751	1.91	30.27	36.99	0.01	0.910	1.31
***bhr*-11 nitrogen neighbourhood**														
narA	nitrate reductase subunit alpha	JT25_RS02985	3735	F	32.81	86.13	1.03	0.000	3.00	35.84	19.24	-0.85	0.000	0.45

narH	nitrate reductase subunit beta	JT25_RS02990	1596	F	42.38	105.88	0.94	0.000	2.91	43.79	25.92	-0.91	0.000	0.39
narJ	nitrate reductase molybdenum cofactor assembly chaperone	JT25_RS02995	720	F	38.92	79.57	0.99	0.000	2.97	32.73	28.02	-0.49	0.000	0.81
narI	respiratory nitrate reductase subunit gamma	JT25_RS03000	678	F	57.48	142.69	1.25	0.000	3.22	59.90	36.01	-0.99	0.000	0.31
	multicopper oxidase Domain-containing protein	JT25_RS03005	1059	F	26.22	69.79	1.16	0.000	3.13	31.77	22.32	-0.23	0.082	1.07
	hypothetical protein	JT25_RS03010	219	F	97.95	199.99	1.74	0.000	3.72	128.30	61.83	-0.63	0.000	0.67
bhr-11	hemerythrin domain-containing protein	JT25_RS03015	333	F	38.22	62.58	1.17	0.000	3.15	75.47	23.55	-1.14	0.000	0.16
	HPP family protein	JT25_RS03020	1185	F	45.08	54.54	0.57	0.000	2.55	33.86	44.21	0.12	0.188	1.42
	NAD(P)/FAD-dependent oxidoreductase	JT25_RS03025	1230	R	51.21	66.18	0.05	0.568	2.03	39.95	36.87	0.43	0.000	1.73
phzF	PhzF family phenazine Biosynthesis protein	JT25_RS03030	921	R	50.59	61.40	0.04	0.707	2.02	20.63	31.09	0.31	0.013	1.61
nirD	nitrite reductase small subunit D	JT25_RS03035	336	R	40.85	50.84	0.41	0.008	2.39	18.39	28.08	0.32	0.133	1.62
nirB	nitrite reductase large subunit B	JT25_RS03040	2541	R	21.28	55.98	0.75	0.000	2.72	14.80	11.33	0.56	0.000	1.86
	formate/nitrite transporter family protein	JT25_RS03045	810	F	22.93	130.56	2.08	0.000	4.06	8.05	5.42	-0.82	0.001	0.48
	bifunctional protein-serine/threonine kinase/phosphatase	JT25_RS03050	1851	F	14.22	46.66	1.34	0.000	3.32	5.07	5.22	-0.24	0.235	1.06
narK	NarK family nitrate/nitrite MFS transporter	JT25_RS03055	1476	F	7.48	10.10	0.91	0.000	2.89	1.86	2.42	0.10	0.772	1.41

***bhr*-66 sensing neighborhood**

lexA	transcriptional repressor LexA	JT25_RS17770	618	R	6.57	12.02	0.62	0.103	2.60	10.07	8.74	-0.49	0.053	0.81

	response regulator	JT25_RS17775	807	R	21.14	25.57	0.01	0.965	1.99	24.80	22.30	-0.42	0.003	0.88
	DUF447 family protein	JT25_RS17780	564	F	132.49	242.09	0.71	0.000	2.68	155.51	222.25	0.64	0.000	1.94
	hypothetical protein	JT25_RS17785	687	F	100.03	139.33	0.36	0.000	2.34	97.49	123.79	0.06	0.453	1.36
	EAL domain-containing protein	JT25_RS17790	3303	F	52.09	49.09	-0.25	0.000	1.73	66.52	44.21	-0.26	0.000	1.04
	AEC family transporter	JT25_RS17795	924	F	52.51	36.70	-0.56	0.000	1.42	40.93	42.50	-0.22	0.021	1.08
	competence/damage-inducible protein A	JT25_RS17800	1227	F	16.21	18.39	0.09	0.694	2.07	22.13	19.04	0.24	0.091	1.54
	ATP-binding cassette domain-containing protein	JT25_RS17805	1887	F	35.74	43.64	0.03	0.822	2.01	53.44	44.50	-0.19	0.004	1.11
	hypothetical protein	JT25_RS17810	420	R	68.69	73.58	0.09	0.633	2.07	68.77	68.53	-0.25	0.027	1.05
bhr-66	bacteriohemerythrin	JT25_RS17815	1785	F	48.44	63.83	0.28	0.002	2.26	45.44	53.34	0.17	0.013	1.47
	response regulator	JT25_RS17820	1320	F	39.68	45.03	-0.05	0.763	1.93	41.03	38.23	-0.04	0.706	1.26
ppk2	polyphosphate kinase 2	JT25_RS17825	783	F	36.87	50.14	0.49	0.002	2.47	37.17	47.23	0.07	0.542	1.37
	hypothetical protein	JT25_RS17830	645	R	86.78	75.61	-0.24	0.072	1.74	111.16	110.81	0.23	0.003	1.53
	hypothetical protein	JT25_RS17835	2244	R	55.70	67.73	0.19	0.013	2.17	91.41	123.89	0.50	0.000	1.80
	hypothetical protein	JT25_RS17840	1140	R	7.31	17.17	0.83	0.003	2.80	9.25	13.59	0.27	0.113	1.57
	hypothetical protein	JT25_RS17845	561	F	1.96	1.29	-0.23	0.782	1.75	1.00	1.59	0.30	0.596	1.60
gspD	type II secretion system secretin GspD	JT25_RS17850	1908	F	1.38	4.89	0.83	0.230	2.81	0.85	1.14	0.18	0.682	1.48
gspE	type II secretion system ATPase GspE	JT25_RS17855	1512	F	1.27	2.08	0.21	0.743	2.19	0.95	1.57	0.35	0.409	1.66
***bhr*-77, *bhr*-88 chemotaxis neighbourhood**														
	chemotaxis response regulator protein-glutamate methylesterase	JT25_RS18665	1095	R	44.02	103.47	1.08	0.000	3.06	46.36	64.11	0.54	0.000	1.84
cheD	chemotaxis protein CheD	JT25_RS18670	597	R	34.68	163.80	1.96	0.000	3.94	70.61	80.00	0.33	0.001	1.63
cheR	Protein-glutamate O-methyltransferase	JT25_RS18675	807	R	58.08	199.36	1.55	0.000	3.53	53.85	101.73	0.65	0.000	1.95

	hypothetical protein	JT25_RS18680	1209	F	186.80	602.19	1.59	0.000	3.57	196.48	406.79	0.92	0.000	2.22
	response regulator	JT25_RS18685	369	F	312.41	1,079.75	1.64	0.000	3.62	417.07	749.70	1.04	0.000	2.34
	STAS domain-containing protein	JT25_RS18690	333	F	214.74	532.60	1.21	0.000	3.19	238.96	386.06	0.87	0.000	2.17
cheA	chemotaxis protein CheA	JT25_RS18695	2202	F	127.43	297.19	1.08	0.000	3.06	111.08	191.32	0.52	0.000	1.82
	HAMP domain-containing protein	JT25_RS18700	2034	F	176.46	453.17	1.21	0.000	3.19	200.61	324.35	0.71	0.000	2.02
cheW	purine-binding chemotaxis protein CheW	JT25_RS18705	546	F	209.45	446.22	0.99	0.000	2.97	297.34	336.69	0.41	0.000	1.71
bhr-77	bacteriohemerythrin	JT25_RS18710	405	R	107.16	176.26	0.62	0.000	2.60	146.80	119.38	0.07	0.470	1.37
bhr-88	hemerythrin family protein	JT25_RS18715	414	R	50.66	80.73	0.59	0.000	2.57	64.90	73.10	0.22	0.071	1.52
	methyl-accepting chemotaxis protein	JT25_RS18720	1878	R	21.25	39.93	0.51	0.001	2.49	24.06	33.64	0.23	0.007	1.53
	formate--tetrahydrofolate ligase	JT25_RS18725	1674	R	61.58	69.40	0.13	0.181	2.11	82.37	74.66	-0.29	0.000	1.01

Normalization

rpoB	DNA-directed RNA polymerase Subunit beta	JT25_RS14695	4077	F	418.02	113.34	-1.98	0.000		421.34	162.99	-1.30	0.000	

Figure Legends

Figure 1. Unroooted phylogram of prokaryotic genes related to the 10 *bhr* genes from *M. denitrificans* FJG1. Homologues were identified from the GenBank database using BLASTn (Geneious Prime 2019 v1.2.3). Scale bar and branch labels represent patristic distances. Sequences from *M. denitrificans* FJG1 are highlighted in pink and genes from other proteobacterial methanotrophs are highlighted in blue.

Figure 2. Cladogram of full-length CDSs matching the *bhr*-66 gene of *M. denitrificans* FJG1 (rooted with eukaryotic outgroup *Themiste pyroides* (KY007473 – KY007479; Geneious Prime 2019 v1.2.3). Scale bar indicates the number of substitutions per site. Green font: Betaproteobacteria, red font: Gammaproteobacteria, blue font: Alphaproteobacteria, purple font: Actinobacteria. Genes from methanotrophic organisms are highlighted in pink.

Figure 3. Cladograms of phylogenetic pairings between *bhr*-00 and *bhr*-66 with 16S rRNA genes in methanotrophs and of *bhr*-00 with *bhr*-99 genes (Geneious Prime 2019 v1.2.3). Yellow highlights indicate multiple branch differences, green highlights indicates one branch difference, and blue highlights indicate consistent branch topology.

Figure 4. Gene neighbourhoods and colour-coded gene annotations surrounding *bhr*-00, *bhr*-66, and *bhr*-99 (Geneious Prime 2019 v1.2.3). Key genes were colour-coded to discriminate functional categories. ***bhr*-00** Orange: Bacteriohemerythrin, Hot pink: Biotin, Light pink: Cytochrome, Purple: Signaling, Gray: Hypothetical. **bhr-66** Orange: Bacterioemerythrin, Light pink: Cytochrome, Light blue: Response regulator, Purple: EAL, Teal: Two-component

regulatory system, Green: Type II secretion, Gray: Hypothetical. **bhr-99**, Orange: Bacteriohemerythrin, Hot pink: Sulfite reductase, Sea green: Na^+ transport, Purple: AlkB dioxygenase, Green: Efflux, Gray: Hypothetical.

Figure 5. Gene neighbourhoods with differential gene expression in high versus low oxygen for *M. denitrificans* FJG1 grown in AMS (left) or NMS (right) medium. Blue highlights indicate downregulation and red highlights indicate upregulation of gene expression. Range of differential expression in AMS varies from -4.15 to 7.29, and range of differential expression in NMS varies from -5.41 to 7.95. Tables 2 and 3 contain actual expression data.

Figure 6. AlphaFold2 Predicted Protein Structures visualized in Mol* Viewer. **A.** Bhr protein structures predicted from *M. denitrificans* FJG1 genes from the AlphaFold2 database. Br-55 was not found using AlphaFold2 and was instead created using Robetta, as described in Methods. **B.** Structural comparison of predicted AlphaFold2 structure for Bhr-00 (ID: A0A140E3I1) with experimentally determined Bhr-Bath structure (8)(PDB ID: 4XPX). Diiron cofactor is shown in orange. Animated superposition in .mp4 format is available in Supplemental files.

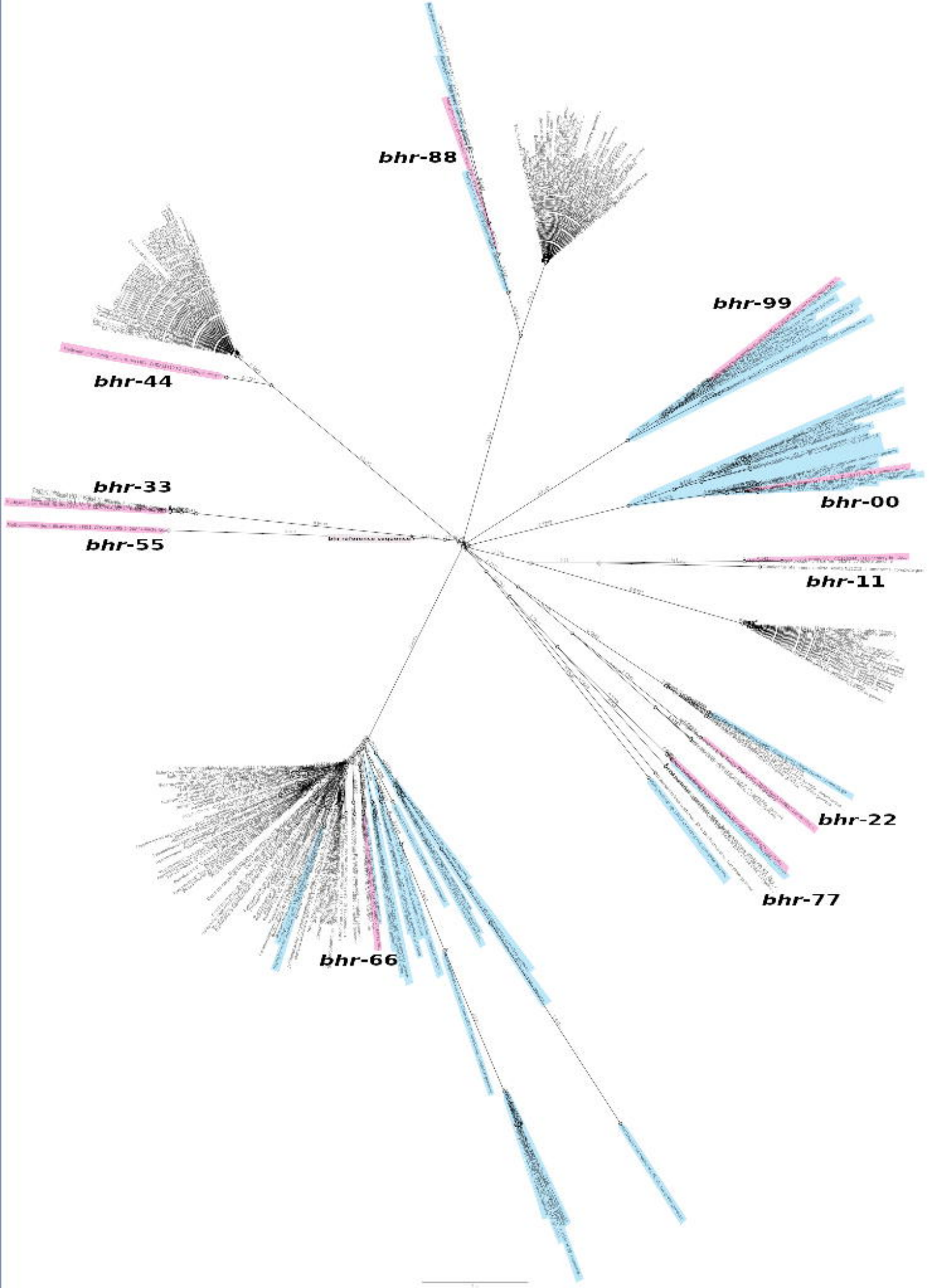
bhr-88
bhr-99
bhr-44
bhr-33
bhr-00
bhr-55
bhr-11
bhr-22
bhr-77
bhr-66

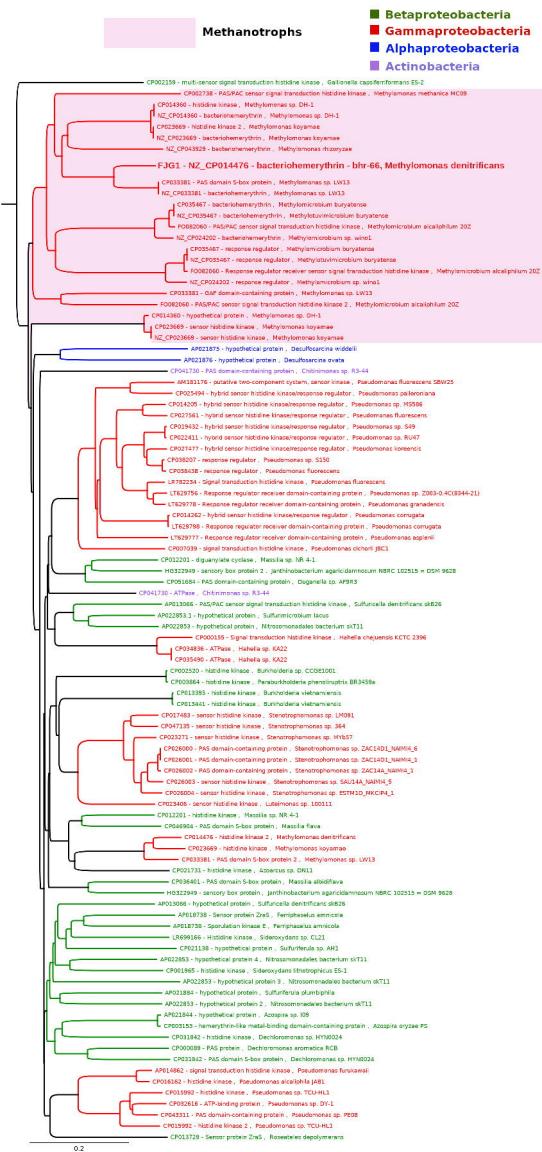
Methanotrophs
Betaproteobacteria
Gammaproteobacteria
Alphaproteobacteria
Actinobacteria
CP002159 - multi-sensor signal transduction histidine kinase , Gallionella capsiferriformans ES-2
CP002738 - PAS/PAC sensor signal transduction histidine kinase , Methylomonas methanica MC09
CP014360 - histidine kinase , Methylomonas sp. DH-1
NZ_CP014360 - bacteriohemerythrin , Methylomonas sp. DH-1
CP023669 - histidine kinase 2 , Methylomonas koyamae
NZ_CP023669 - bacteriohemerythrin , Methylomonas koyamae
NZ_CP043929 - bacteriohemerythrin , Methylomonas rhizoryzae
FJG1 - NZ_CP014476 - bacteriohemerythrin - bhr-66, Methylomonas denitrificans
CP033381 - PAS domain S-box protein , Methylomonas sp. LW13
NZ_CP033381 - bacteriohemerythrin , Methylomonas sp. LW13
CP035467 - bacteriohemerythrin , Methylomicrobium buryatense
NZ_CP035467 - bacteriohemerythrin , Methylotuvimicrobium buryatense
FO082060 - PAS/PAC sensor signal transduction histidine kinase , Methylomicrobium alcalophilum 20Z
NZ_CP024202 - bacteriohemerythrin , Methylomicrobium sp. wine1
CP035467 - response regulator , Methylomicrobium buryatense
NZ_CP035467 - response regulator , Methylotuvimicrobium buryatense
FO082060 - Response regulator receiver sensor signal transduction histidine kinase , Methylomicrobium alcalophilum 20Z
NZ_CP024202 - response regulator , Methylomicrobium sp. wine1
CP033381 - GAF domain-containing protein , Methylomonas sp. LW13
FO082060 - PAS/PAC sensor signal transduction histidine kinase 2 , Methylomicrobium alcalophilum 20Z
CP014360 - hypothetical protein , Methylomonas sp. DH-1
CP023669 - sensor histidine kinase , Methylomonas koyamae
NZ_CP023669 - sensor histidine kinase , Methylomonas koyamae
AP021875 - hypothetical protein , Desulfosarcina widdelii
AP021876 - hypothetical protein , Desulfosarcina ovata
CP041730 - PAS domain-containing protein , Chitinimonas sp. R3-44
AM181176 - putative two-component system, sensor kinase , Pseudomonas fluorescens SBW25
CP025494 - hybrid sensor histidine kinase/response regulator , Pseudomonas palleroniana
CP014205 - hybrid sensor histidine kinase/response regulator , Pseudomonas sp. H5B66
CP027561 - hybrid sensor histidine kinase/response regulator , Pseudomonas fluorescens
CP019432 - hybrid sensor histidine kinase/response regulator , Pseudomonas sp. S49
CP022411 - hybrid sensor histidine kinase/response regulator , Pseudomonas sp. RU47
CP027477 - hybrid sensor histidine kinase/response regulator , Pseudomonas koreensis
CP038207 - response regulator , Pseudomonas sp. S150
CP038638 - response regulator , Pseudomonas fluorescens
LR782234 - Signal transduction histidine kinase , Pseudomonas fluorescens
LT629756 - Response regulator receiver domain-containing protein , Pseudomonas sp. ZO63-0-4C(8344-21)
LT629778 - Response regulator receiver domain-containing protein , Pseudomonas granadensis
CP014262 - hybrid sensor histidine kinase/response regulator , Pseudomonas chlororaphis
LT628798 - Response regulator receiver domain-containing protein , Pseudomonas corrugata
LT629777 - Response regulator receiver domain-containing protein , Pseudomonas aeginensis
CP007039 - signal transduction histidine kinase , Pseudomonas cichorii JBC1
CP012201 - diguanylate cyclase , Massilia sp. NR 4-1
HG322949 - sensory box protein 2 , Janthinobacterium agaricidamnosum NBRC 102515 = DSM 9628
CP016864 - PAS domain-containing protein , Duganella sp. AP3R3
CP041730 - ATPase , Chitinimonas sp. R3-44
AP013066 - PAS/PAC sensor signal transduction histidine kinase , Sulfuricella denitrificans skB26
AP022853.1 - hypothetical protein , Sulfuriricmicrobium lacus
AP022853 - hypothetical protein , Nitrosomonadales bacterium sk711
CP000155 - Signal transduction histidine kinase , Hahella chejuensis KCTC 2396
CP034836 - ATPase , Hahella sp. KA22
CP035490 - ATPase , Hahella sp. KA22
CP002520 - histidine kinase , Burkholderia sp. CCGE1001
CP003864 - histidine kinase , Paraburkholderia phenylfuglebs BR3459a
CP013395 - histidine kinase , Burkholderia vietnamensis
CP013441 - histidine kinase , Burkholderia vietnamensis
CP017483 - sensor histidine kinase , Stenotrophomonas sp. LM091
CP047135 - sensor histidine kinase , Stenotrophomonas sp. J64
CP023271 - sensor histidine kinase , Stenotrophomonas sp. HY557
CP026000 - PAS domain-containing protein , Stenotrophomonas sp. ZAC14D1_NAIM14_6
CP026001 - PAS domain-containing protein , Stenotrophomonas sp. ZAC14D1_NAIM14_3
CP026002 - PAS domain-containing protein , Stenotrophomonas sp. ZAC14A_NAIM14_1
CP026003 - sensor histidine kinase , Stenotrophomonas sp. SAU14A_NAIM14_5
CP026004 - sensor histidine kinase , Stenotrophomonas sp. ESTM1D_MKC1P4_1
CP023408 - sensor histidine kinase , Luteimonas sp. 100111
CP012201 - histidine kinase , Massilia sp. NR 4-1
CP040904 - PAS domain S-box protein , Massilia flava
CP014476 - histidine kinase 2 , Methylomonas denitrificans
CP023669 - histidine kinase , Methylomonas koyamae
CP033381 - PAS domain S-box protein 2 , Methylomonas sp. LW13
CP021731 - histidine kinase , Azoarcus sp. DN11
CP036401 - PAS domain S-box protein , Massilia albidiflava
HG322949 - sensory box protein , Janthinobacterium agaricidamnosum NBRC 102515 = DSM 9628
AP013066 - hypothetical protein , Sulfuricella denitrificans skB26
AP018738 - Sensor protein ZraS , Ferriphaselus amnicola
AP018738 - Sporulation kinase E , Ferriphaselus amnicola
LR699166 - Histidine kinase , Sideroxydans sp. CL21
CP021138 - hypothetical protein , Sulfuriflexus sp. AH1
AP022853 - hypothetical protein 4 , Nitrosomonadales bacterium sk711
CP001965 - histidine kinase , Sideroxydans lithotrophicus ES-1
AP022853 - hypothetical protein 3 , Nitrosomonadales bacterium sk711
AP021864 - hypothetical protein , Sulfuriferula plumbiphila
AP022853 - hypothetical protein 2 , Nitrosomonadales bacterium sk711
AP021844 - hypothetical protein , Azospira sp. I09
CP003153 - hemerythrin-like metal-binding domain-containing protein , Azospira oryzae PS
CP031842 - histidine kinase , Dechloromonas sp. HYM0024
CP006089 - PAS protein , Dechloromonas aromatica RCB
CP031842 - PAS domain S-box protein , Dechloromonas sp. HYM0024
AP014862 - signal transduction histidine kinase , Pseudomonas furukawaii
CP016162 - histidine kinase , Pseudomonas alcaligenes JAB1
CP015992 - histidine kinase , Pseudomonas sp. TCU-HL1
CP032616 - ATP-binding protein , Pseudomonas sp. DT-1
CP043311 - PAS domain-containing protein , Pseudomonas sp. PE08
CP015992 - histidine kinase 2 , Pseudomonas sp. TCU-HL1
CP013729 - Sensor protein ZraS , Roseateles depolymerans
0.2

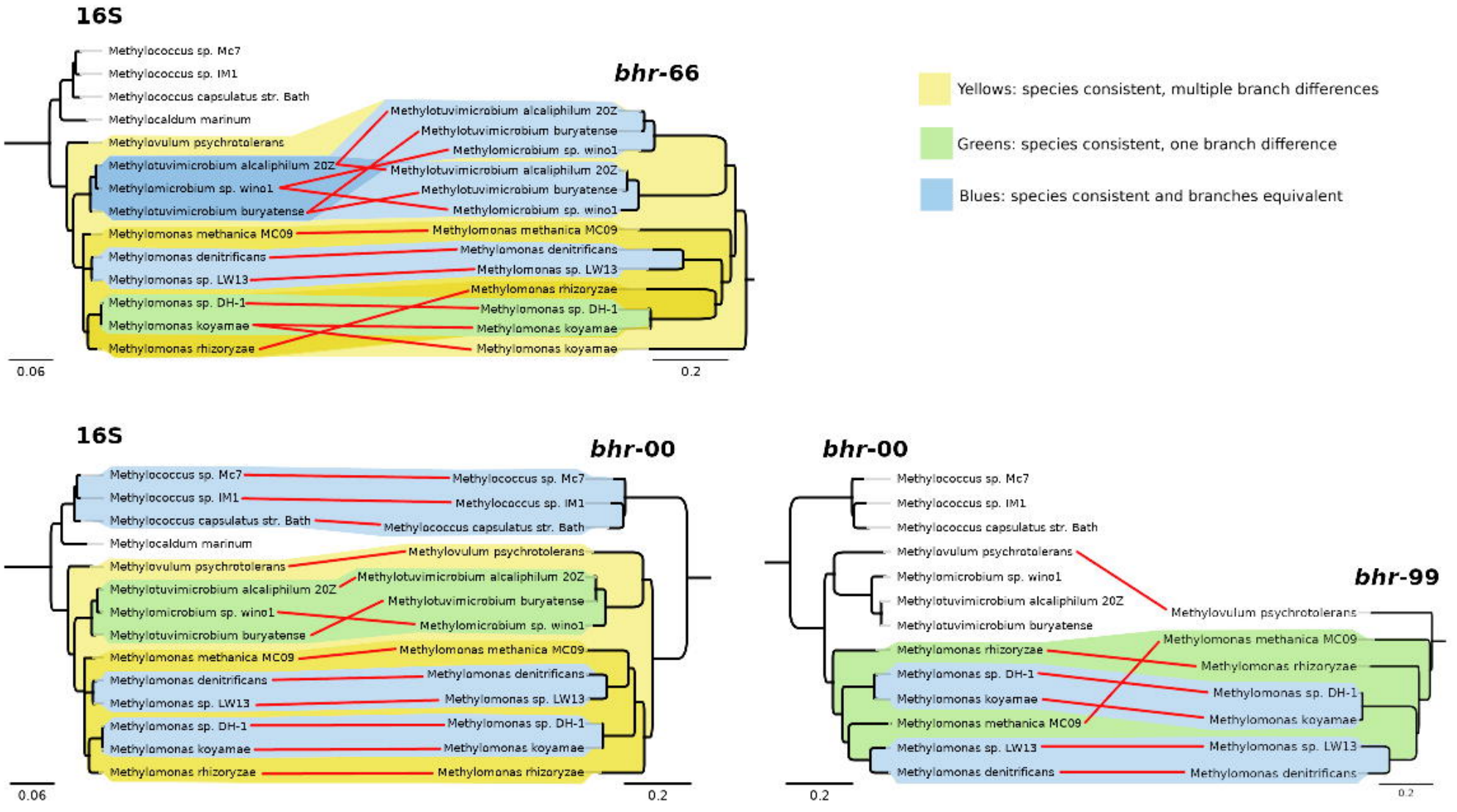
16S
bhr-66
Methylococcus sp. Mc7
Methylococcus sp. IM1
Methylococcus capsulatus str. Bath
Methylocaldum marinum
Methylovulum psychrotolerans
Methylotuvimicrobium alcaliphilum 20Z
Methylomicrobium sp. wino1
Methylotuvimicrobium buryatense
Methylomonas methanica MC09
Methylomonas denitrificans
Methylomonas sp. LW13
Methylomonas sp. DH-1
Methylomonas koyamae
Methylomonas rhizoryzae
Methylotuvimicrobium alcaliphilum 20Z
Methylotuvimicrobium buryatense
Methylomicrobium sp. wino1
Methylotuvimicrobium alcaliphilum 20Z
Methylotuvimicrobium buryatense
Methylomicrobium sp. wino1
Methylomonas methanica MC09
Methylomonas denitrificans
Methylomonas sp. LW13
Methylomonas rhizoryzae
Methylomonas sp. DH-1
Methylomonas koyamae
Methylomonas koyamae
0.06
0.2
Yellows: species consistent, multiple branch differences
Greens: species consistent, one branch difference
Blues: species consistent and branches equivalent
16S
bhr-00
Methylococcus sp. Mc7
Methylococcus sp. IM1
Methylococcus capsulatus str. Bath
Methylocaldum marinum
Methylovulum psychrotolerans
Methylotuvimicrobium alcaliphilum 20Z
Methylomicrobium sp. wino1
Methylotuvimicrobium buryatense
Methylomonas methanica MC09
Methylomonas denitrificans
Methylomonas sp. LW13
Methylomonas sp. DH-1
Methylomonas koyamae
Methylomonas rhizoryzae
Methylococcus sp. Mc7
Methylococcus sp. IM1
Methylococcus capsulatus str. Bath
Methylovulum psychrotolerans
Methylotuvimicrobium alcaliphilum 20Z
Methylotuvimicrobium buryatense
Methylomicrobium sp. wino1
Methylomonas methanica MC09
Methylomonas denitrificans
Methylomonas sp. LW13
Methylomonas sp. DH-1
Methylomonas koyamae
Methylomonas rhizoryzae
0.06
0.2
bhr-00
Methylococcus sp. Mc7
Methylococcus sp. IM1
Methylococcus capsulatus str. Bath
Methylovulum psychrotolerans
Methylomicrobium sp. wino1
Methylotuvimicrobium alcaliphilum 20Z
Methylotuvimicrobium buryatense
Methylomonas rhizoryzae
Methylomonas sp. DH-1
Methylomonas koyamae
Methylomonas methanica MC09
Methylomonas sp. LW13
Methylomonas denitrificans
bhr-99
Methylovulum psychrotolerans
Methylomonas methanica MC09
Methylomonas rhizoryzae
Methylomonas sp. DH-1
Methylomonas koyamae
Methylomonas sp. LW13
Methylomonas denitrificans
0.2
0.2

bhr-00
Orange: Hemerythrin
Hot pink: Biotin
Light pink: Cytochrome
Purple: Signaling
Gray: Hypothetical
Methylomonas denitrificans
Methylomonas denitrificans
Methylomonas sp. LW13
Methylomonas koyamae
Methylomonas sp. DH-1
Methylomonas rhizoryzae
Methylomonas methanica MC09
Methylomicrobium sp. wino1
Methylotuvimicrobium buryatense
Methylotuvimicrobium alcaliphilum 20Z
Methylococcus sp. IM1
Methylovulum psychrotolerans
bhr-66
Orange: Hemerythrin
Light pink: Cytochrome
Light blue: Response regulator
Purple: EAL
Teal: Two-component
Green: Type II secretion
Gray: Hypothetical
bhr-99
Orange: Hemerythrin
Hot pink: Sulfite
Sea green: Na+ transport
Purple: AlkB dioxygenase
Green: Efflux
Gray: Hypothetical

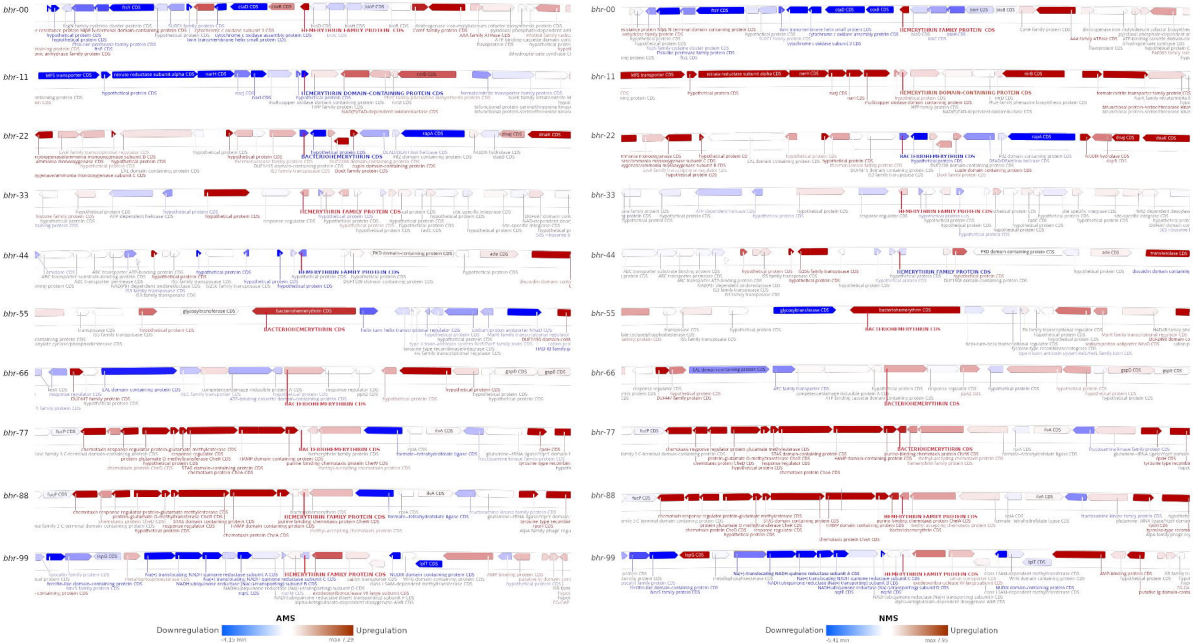
bhr-00
bhr-11
bhr-22
bhr-33
bhr-44
bhr-55
bhr-66
bhr-77
bhr-88
bhr-99
HEMERYTHRIN FAMILY PROTEIN CDS
HEMERYTHRIN DOMAIN-CONTAINING PROTEIN CDS
BACTERIOHEMERYTHRIN CDS
AMS
Downregulation
Upregulation
-4.15 min
max 7.29
NMS
Downregulation
Upregulation
-5.41 min
max 7.95

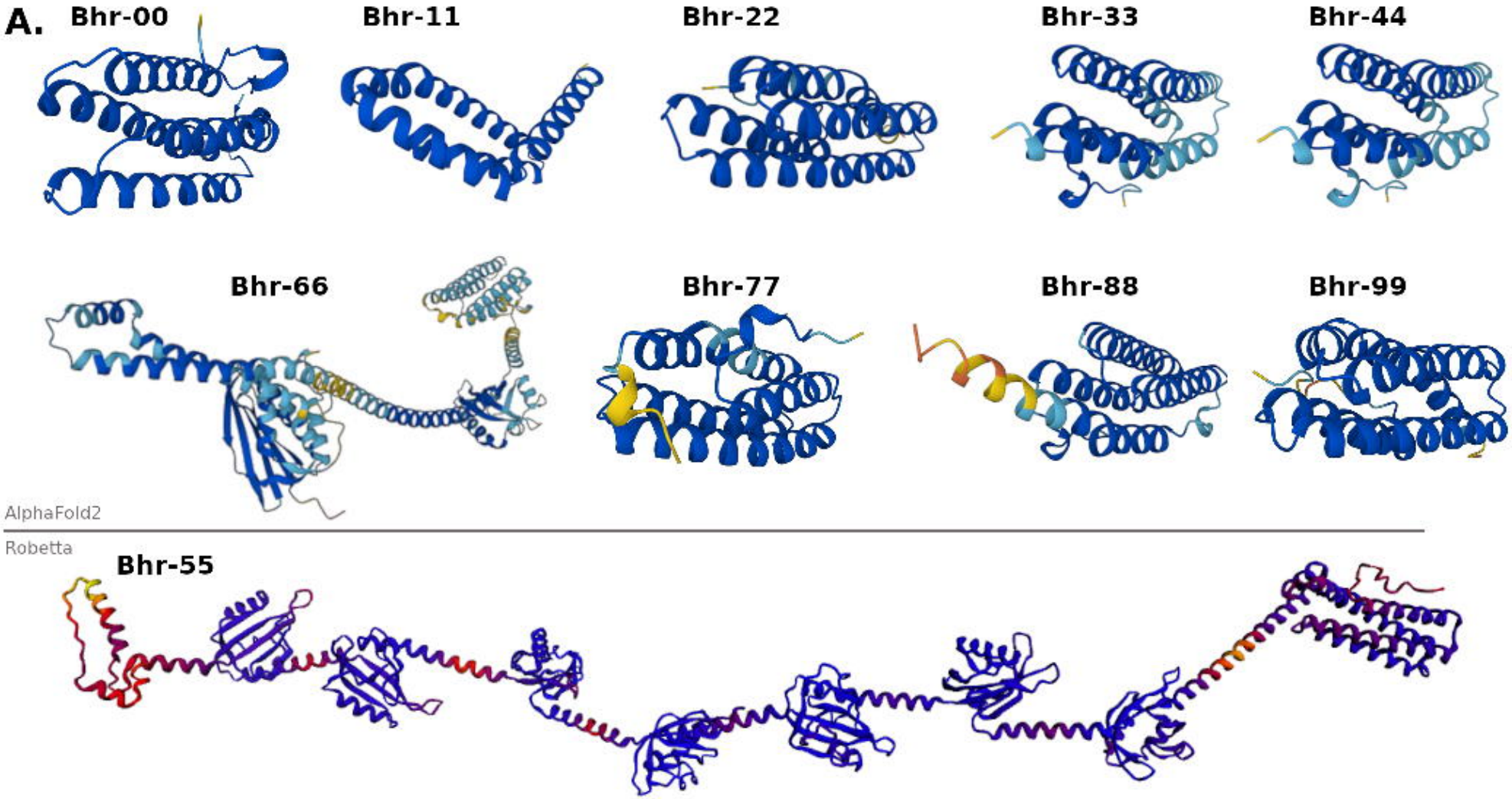
A.
Bhr-00
Bhr-11
Bhr-22
Bhr-33
Bhr-44
Bhr-66
Bhr-77
Bhr-88
Bhr-99
AlphaFold2
Robetta
Bhr-55

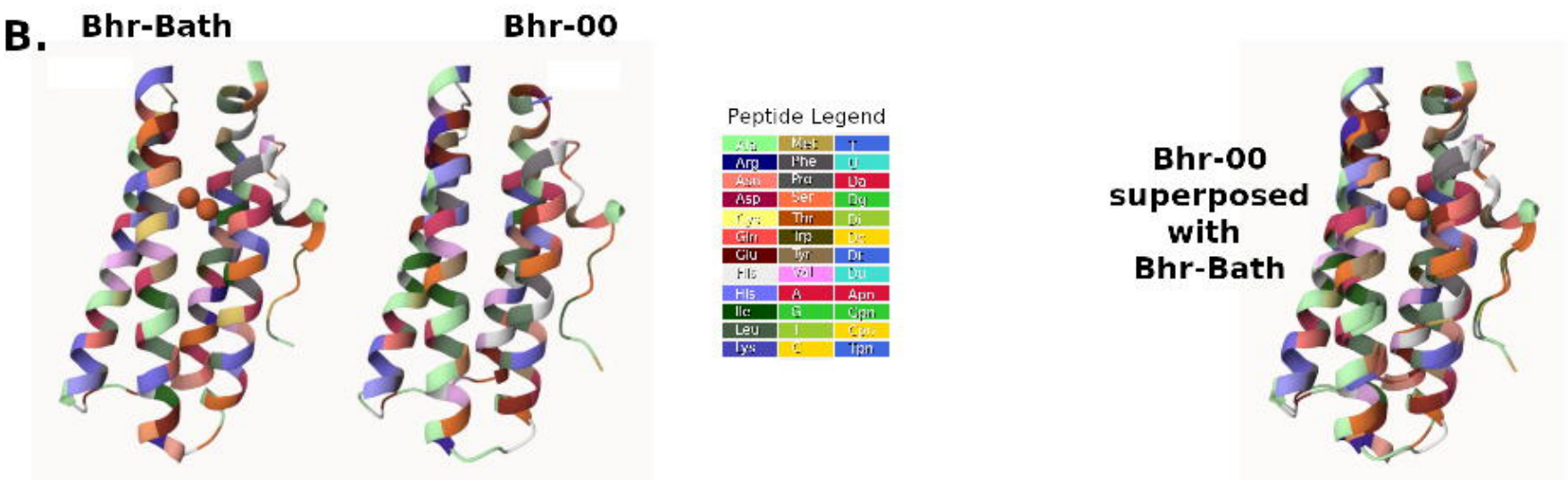
B.
Bhr-Bath
Bhr-00
Peptide Legend
Bhr-00
superposed
with
Bhr-Bath